Coordination Chemistry Reviews
Elsevier Publishing Company Amsterdam
Printed in The Netherlands

THE VISIBLE AND ULTRAVIOLET SPECTRA OF d^6-, d^7- AND d^8-METAL IONS IN TRIGONAL BIPYRAMIDAL COMPLEXES

M. J. NORGETT, J. H. M. THORNLEY AND L. M. VENANZI

Clarendon and Inorganic Chemistry Laboratories, University of Oxford (Great Britain)

Transition metal complexes with co-ordination number five and trigonal bipyramidal structure are not very common. The most extensive series of complexes of this type have been obtained using multidentate ligands. Thus, the polyamine $N(CH_2CH_2NMe_2)_3$ gives trigonal bipyramidal complexes with chromium(II), manganese(II), iron(II), cobalt(II), nickel(II), copper(II) and zinc(II)[1]. The metal ions are present in the high-spin form for electronic configurations d^4 to d^8. Phosphorus-, and arsenic-containing ligands, on the other hand such as tris(*o*-diphenylphosphinophenyl)phosphine, QP and its arsenic analogue QAS, give trigonal bipyramidal complexes

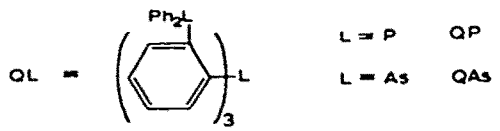

with a wide range of metal ions in their low-spin form of the types [MX(QL)], $[ML(QL)]^+$, $[MX(QL)]^+$ and $[ML(QL)]^{2+}$ (X = anionic ligand, L = uncharged ligand, QL = QP or QAS)[2]. A selection of the compounds of the above types prepared to date is shown in Table 1.

The visible and ultraviolet spectra of these complexes have one common characteristic: the molar extinction coefficients of the low-energy bands are very high ranging between 500 and 8000 (see Figs. 1, 2, 3, 4 and 5). The most obvious assignment for bands with such high intensities is that they are due to charge transfer processes and this possibility has been considered by Jørgensen[3]. It is, however, likely that they are predominantly "ligand-field" bands for the following reasons:

1. High intensity, low-energy bands are observed in complexes of phosphorus and arsenic ligands with octahedral structure of the type $[M^{n+}X_2(QL)]^{(n-2)+}$ (Ref. 4). The range of complexes examined is given in Table 2. Of particular interest in this connection is the comparison between the absorption bands of complexes of chromium(III) and cobalt(III) with nitrogen and with phosphorus ligands. The relevant data are given in Table 3. Here the close analogy of the band

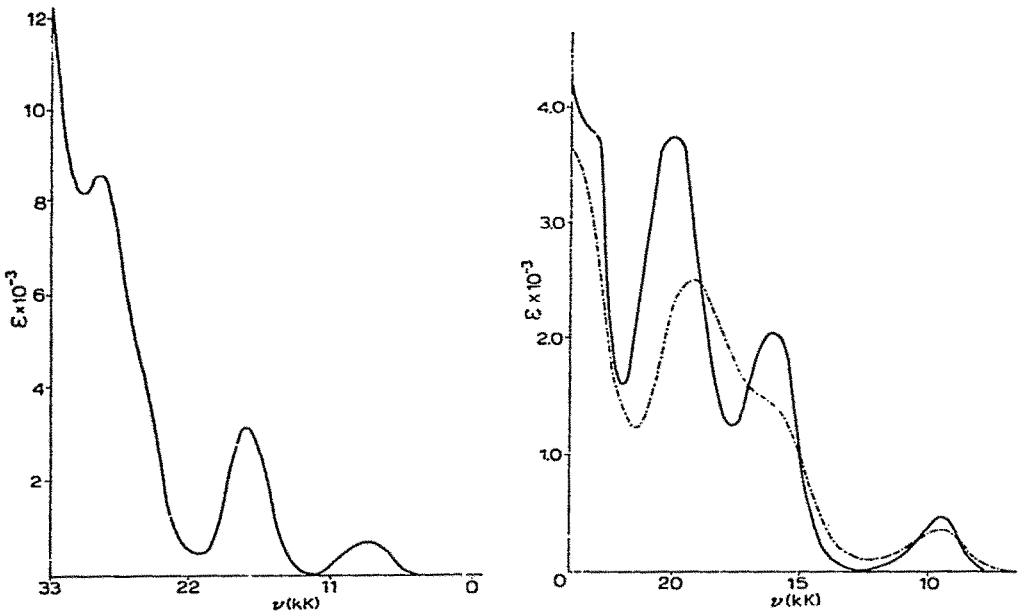

Fig. 1. The visible and ultraviolet spectrum of [FeBr(QP)] [BPh_4] in dichloromethane solution.
Fig. 2. The visible and ultraviolet spectrum of [CoBr(QP)] [BPh_4], .–.–, at room temperature in dichloromethane solution; ———, at liquid nitrogen temperature in a tetrahydrofurfuryl alcohol glass.

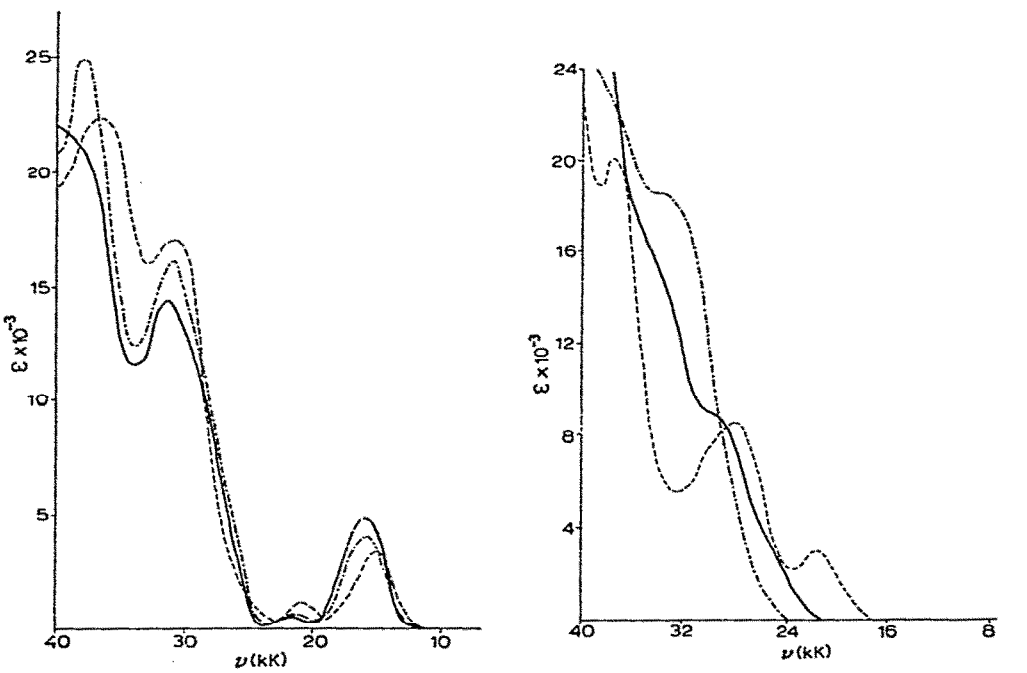

Fig. 3. The visible and ultraviolet spectra of complexes [NiX(QAS)](ClO_4) in dichloromethane solution. ———, X = Cl; – – –, X = Br; .–.–, X = I.
Fig. 4. The visible and ultraviolet spectra of complexes [M(CO) (QAS)] in dichloromethane solution. – – –, M = Co; ———, M = Rh; .–.–, M = Ir.

TABLE 1

COLOUR, DECOMPOSITION POINT, MOLAR CONDUCTANCE AND MAGNETIC MOMENT OF FIVE-CO-ORDINATE COMPLEXES OF QP AND QAS

Compound	*Colour*	*Decomp. p. (°C)*	Λ_M[a]	$\mu_{eff.}$	*Refer.*
[FeCl(QP)] [BPh_4]	dark violet	246–250	15.0	3.04	8
[FeBr(QP)] [BPh_4]	blue-black	248–253	14.8	3.03	8
[FeI(QP)] [BPh_4]	green-black	258–262	14.6	3.08	8
[Co(CO) (QAS)] [BPh_4]	red-orange	232–234	15.1	diamag.	9
[Rh(CO) (QAS)] Cl	yellow	222–225	22.1	diamag.	10
[Ir(CO) (QAS)] [BPh_4]	yellow	272–279	16.9	diamag.	11
[RhCl(QAS)]	red-purple	>330	0.3	diamag.	10
[RhBr(QAS)]	deep-purple	>330	0.2	diamag.	10
[RhI(QAS)]	dark purple	>330	0.1	diamag.	10
[CoCl(QP)] [BPh_4]	red-black	262–263	15.2	1.99	12
[CoBr(QP)] [BPh_4]	blue-black	258–259	14.9	1.98	12
[CoI(QP)] [BPh_4]	blue-black	265–267	14.6	1.94	12
[NiCl(QP)] (ClO_4)	deep purple	353–356	22.7	diamag.	13
[NiCl(QAS)] (ClO_4)	dark blue	321–322	23.9	diamag.	13
[NiBr(QAS)] (ClO_4)	dark blue	321–322	23.0	diamag.	13
[NiI(QAS)] (ClO_4)	blue-black	338–339	23.8	diamag.	13
[PdCl(QAS)]Cl	red-purple	276–279	23.1	diamag.	14
[PdBr(QAS)]Br	deep purple	281–283	17.6	diamag.	14
[PdI(QAS)]I	dark purple	285–287	15.3	diamag.	14
[PtCl(QAS)] [BPh_4]	orange	274–276	17.4	diamag.	15
[PtBr(QAS)] [BPh_4]	deep orange	294–295	18.5	diamag.	15
[PtI(QAS)] [BPh_4]	red	278–279	20.7	diamag.	15
[Pt(thiourea) (QAS)] (ClO_4)$_2$	yellow-orange	344–345	42.8	diamag.	16
[Pt(Me_2S) (QAS)] (ClO_4)$_2$	yellow-orange	349–351	47.1	diamag.	16

[a] In mhos, for 10^{-3} *M* nitrobenzene solutions at 20°.

structure for the complexes allows the assignment of bands in the phosphine complexes.

2. Changes of the anionic ligand in complexes $[NiX(QAS)]^+$ cause very large changes in position of the lowest-energy band, *e.g.*, the difference between X = I and X = CN is 6500 cm^{-1} (see Fig. 6).

3. The low-energy bands in $[NiBr(TSP)]^+$ (TSP = (*o*-Me · S · C_6H_4)$_3$P) which is trigonal bipyramidal have lower intensities than those of analogous $[NiBr(TSeP)]^+$ which are lower than those of $[NiBr(QP)]^+$ while the positions of absorption do not change greatly (see Table 4).

4. It is most unlikely that complexes such as $[MX(QP)]^+$ (M = Fe and Co) have charge transfer bands as low as 10,000 cm^{-1}.

5. The spectra of all the trigonal bipyramidal complexes can be satisfactorily assigned using a "ligand-field" model.

TABLE 2

COLOUR, DECOMPOSITION POINT, MOLAR CONDUCTANCE AND MAGNETIC MOMENT OF SIX-CO-ORDINATE COMPLEXES OF QP AND QAS

Compound	*Colour*	*Decomp.p.(°C)*	Λ_M[a]	$\mu_{eff.}$	*Refer.*
$[CrCl_3(TP)]$	blue	>360	—	3.96	17
$[CrBr_3(TP)]$	blue	>360	—	3.90	17
$[Mn(CO)_3(TP)]Cl$	pale yellow	233–238	24.2	diamag.	18
$[Mn(CO)_3(QP)]Cl$	cream	228–235	25.1	diamag.	18
$[ReCl_3(QAS)]$	orange	278–280	1.3	1.16	19
$[ReCl_3(TAS)]$	red	235–237	0.4	1.60	19
$[Fe(NCS)_2(QP)]$	orange-red	349–351	—	diamag.	8
$[Fe(CN)_2(QP)]$	yellow	>370	—	diamag.	8
$[RuCl_2(QP)]$	yellow	>380	—	diamag.	20
$[OsCl_2(QP)]$	pale yellow	>380	—	diamag.	20
$[CoCl_2(QP)]\,[BPh_4]$	red	198–199	14.7	diamag.	12
$[RhCl_2(QP)]Cl$	yellow	282–285	20.2	diamag.	10
$[RhCl_3(TAS)]$	orange	>330	0.4	diamag.	10
$[IrCl_3(TAS)]$	yellow	328–332	0.5	diamag.	11
$[PdCl_2(QAS)]Cl_2$	yellow	306–310	44.2	diamag.	20
$[PtCl_2(QAS)]Cl_2$	pale yellow	324–328	45.1	diamag.	20

[a] In mhos, for 10^{-3} *M* solutions at 20°.

TABLE 3

ABSORPTION MAXIMA OF COMPLEXES $[CrCl_3L_3]$ AND *cis*-$[CoCl_2(LL)_2]$

Complex	*Transition*	*E*(kK)	log ε	*Reference*
$[CrCl_3py_3]$	$^4T_{2g} \leftarrow {}^4A_{2g}$	15.9	[a]	21
	$^4T_{1g} \leftarrow {}^4A_{2g}$	22.2	[a]	
$[CrCl_3(TP)]$	$^4T_{2g} \leftarrow {}^4A_{2g}$	16.5	3.08	17
	$^4T_{1g} \leftarrow {}^4A_{2g}$	21.0	2.69	
cis-$[CoCl_2(en)_2]^+$	$^1T_{1g} \leftarrow {}^1A_{1g}$	18.6	1.95	22
cis-$[CoCl_2(DAS)_2]^+$	$^1T_{1g} \leftarrow {}^1A_{1g}$	20.4	2.80	22
$[CoCl_2(QP)]^+$	$^1T_{1g} \leftarrow {}^1A_{1g}$	20.3	3.75	12

DAS = 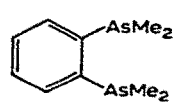

TP = 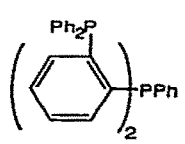

QP = 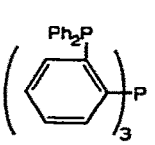

[a] Solid reflection spectrum.

TABLE 4

LIGAND-FIELD BANDS OF TRIGONAL BIPYRAMIDAL COMPLEXES: [NiCl(ligand)]$^+$

Ligand	*Transition*	ν_{max} (cm^{-1})	ε_{max}	*Reference*
(*o*-MeS · C_6H_4)$_3$P	$(e'')^4(e')^4 \rightarrow (e'')^4(e')^3a'_1$	15,390	1260	23
	$(e'')^4(e')^4 \rightarrow (e'')^3(e')^4a'_1$	20,960	303	23
(*o*-MeSe · C_6H_4)$_3$P	$(e'')^4(e')^4 \rightarrow (e'')^4(e')^3a'_1$	15,150	1860	24
	$(e'')^4(e')^4 \rightarrow (e'')^3(e')^4a'_1$	20,300	220	24
(*o*-Ph_2As · C_6H_4)$_3$As	$(e'')^4(e')^4 \rightarrow (e'')^4(e')^3a'_1$	16,200	4470	16
	$(e'')^4(e')^4 \rightarrow (e'')^3(e')^4a'_1$	21,800	330	16
(*o*-Ph_2As · C_6H_4)$_3$P	$(e'')^4(e')^4 \rightarrow (e'')^4(e')^3a'_1$	17,500	4950	16
	$(e'')^4(e')^4 \rightarrow (e'')^3(e')^4a'_1$	[a]	[a]	16

[a] Not resolved.

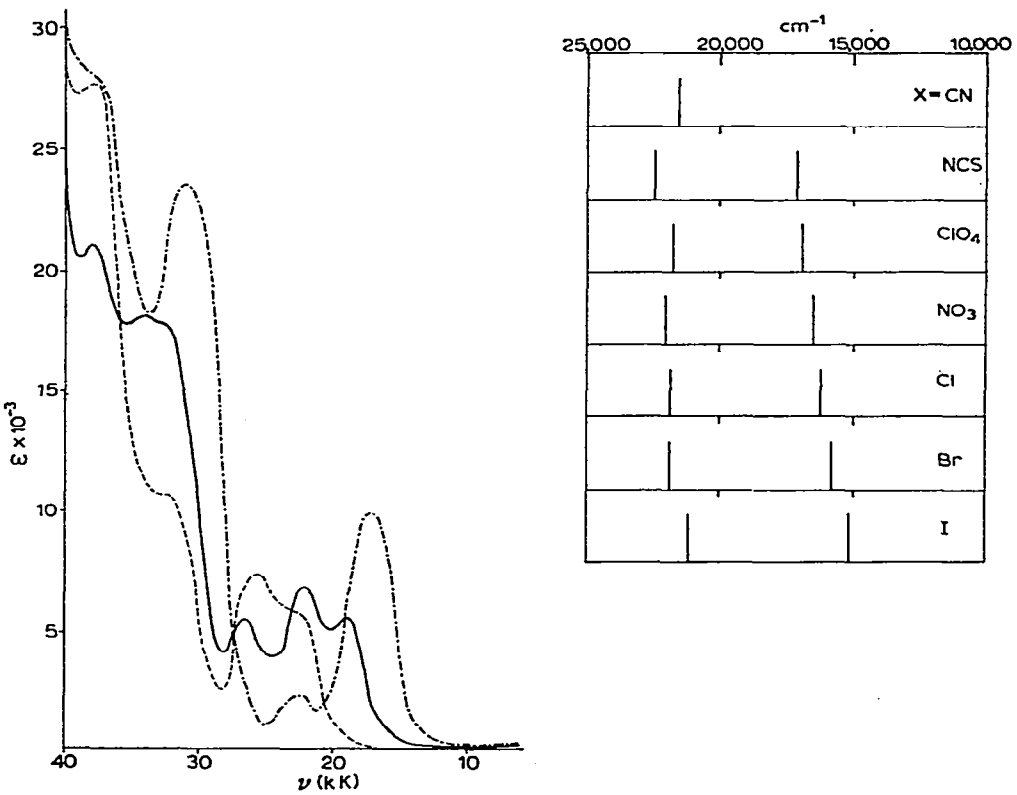

Fig. 5. The visible and ultraviolet spectra of complexes [M(NCS) (QAS)] (ClO_4) in dichloromethane solution. ·–·–·, M = Ni; ———, M = Pd; – – –, M = Pt.

Fig. 6. Band-shifts in compounds [NiX(QAS)](ClO_4). The low-energy band has been assigned to $(e'')^4(e')^4 \rightarrow (e'')^4(e')^3(a'_1)$ transitions and the other to $(e'')^4(e')^4 \rightarrow (e'')^3(e')^4(a'_1)$ transitions.

Crystal-field calculations for trigonal bipyramidal complexes

Tensor operator theory was used to calculate the matrix elements required. The crystal field was expressed in terms of two independent parameters Q_2 and Q_4 defined as indicated in Table 5. The relationship between the one-electron orbital splitting and the parameters Q_2 and Q_4 for D_{3h} and C_{3v} symmetries are also shown in Table 5. The values of Q_2 and Q_4 were not calculated on the basis

TABLE 5

CRYSTAL FIELD PARAMETERS AND TRIGONAL BIPYRAMIDAL FIELDS

$Q_2 = \frac{ge^2\langle r^2\rangle}{R^3}$ $\quad$ $Q_4 = \frac{ge^2\langle r^4\rangle}{R^5}$

g = effective ligand charge $\quad$ e = electronic charge

R = metal-donor atom distance

ψ_{3d} = radial part of the 3d wave-function $\quad$ $\langle r^k\rangle = \int_0^\infty \psi_{3d}^2 r^{(k+2)} dr$

For octahedral complexes: $10Dq = 5/3Q_4$

Orbital splitting	D_{3h}	C_{3v}	d-*functions* *Real orbitals*	*Complex orbitals*	*Orbital energies*[a]
—	a'_1	a_1	z^2	$\|0>$	$1/7\ Q_2+25/28\ Q_4$
—	e'	e_1	x^2-y^2, xy	$\|2>\|-2>$ —	$1/7\ Q_2+25/168\ Q_4$
—	e''	e_2	xz, yz	$\|1>\|-1>$	$1/14\ Q_2-25/42\ Q_4$

[a] The values of Q_2 and Q_4 are weighted mean of contributions from axial and equatorial ligands.

of the physical model used but obtained empirically from spectral data. Energy-level diagrams were obtained in which the energy (in units of B) is plotted against Q_4/B at constant ratios of Q_2/Q_4. A wide range of values of Q_2/Q_4 were tested for each electronic configuration and good qualitative agreement was observed between predicted and observed band-positions and intensities for Q_2/Q_4 over the range 0.5–3.5. The values of Q_2/Q_4 given in the diagrams are those that give the best quantitative fit between the calculated and observed spectra. Finally, in interpreting our energy-level diagrams, it must be borne in mind that intensities are subject to the selection rule $\Delta M_L = \pm 2$ or 3.

Ligand-field bands[5].—For nickel(II) complexes one expects (see Fig. 7) and observes (see Fig. 3) two low-energy bands; the first is due to $(e'')^4(e')^4 \rightarrow (e'')^4(e')^3(a'_1)^1$ and the second due to $(e'')^4(e')^4 \rightarrow (e'')^3(e')^4(a'_1)^1$. Their relative intensities are in accord with the M_L selection rule.

For cobalt(II) complexes one would expect one very low-energy band due to the transition $(e'')^4(e')^3 \rightarrow (e'')^3(e')^4$, three bands due to the transition $(e'')^4(e')^3(a'_1)^1$ and four bands due to $(e'')^4(e')^3 \rightarrow (e'')^3(e')^3(a'_1)^1$ transitions (see Fig. 8).

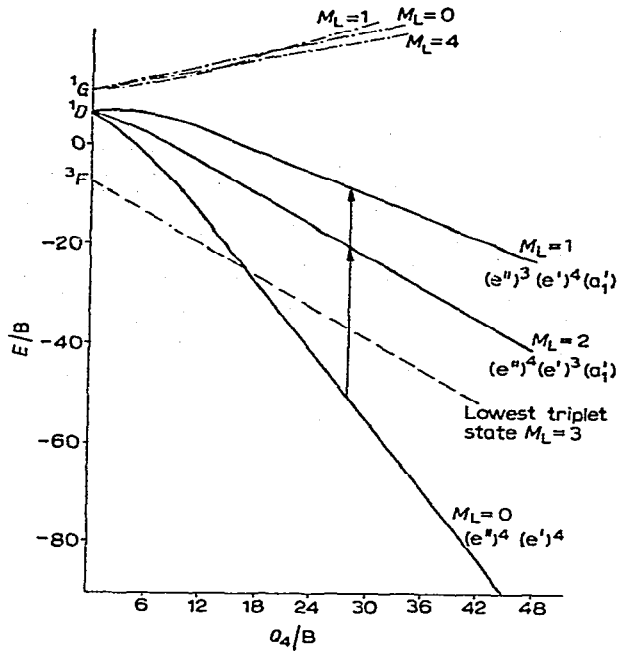

Fig. 7. Energy-level diagram for trigonal-bipyramidal, low-spin complexes of nickel(II), d^8, at $Q_2/Q_4 = 2$. ———, one-electron transitions; .–.–.–., two-electron transitions. (Reproduced by kind permission of the Chemical Society).

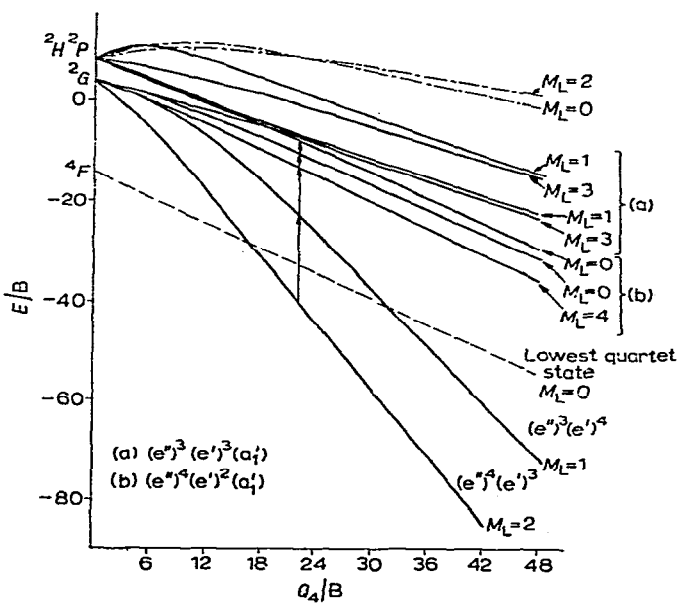

Fig. 8. Energy-level diagram for trigonal-bipyramidal, low-spin complexes of cobalt(II), d^7, at $Q_2/Q_4 = 2.3$. ———, one-electron transitions; .–.–., two electron transitions. (Reproduced by kind permission of the Chemical Society).

The spectra of the complexes (*e.g.* see Fig. 2) show clearly the lowest energy band but, in the region 14,000–24,000 cm^{-1}, only one band and one pronounced shoulder are observed in the room temperature spectra of the complexes. Better resolution is obtained in the spectra of the complexes in glasses at −185° (see Fig. 2). Even in the latter case only two bands are observed in this region. This result is not unexpected as the energy-level diagram indicates that in this region there should be five closely spaced bands.

For the iron(II) complexes one would expect (see Fig. 9) two bands associated with $(e'')^4(e')^2 \rightarrow (e'')^3(e')^3$ transitions, one band associated with $(e'')^4(e')^2 \rightarrow (e'')^4(e')^1(a'_1)^1$ transitions and one band associated with $(e'')^4(e')^2 \rightarrow (e'')^3(e')^2(a'_1)^1$ transitions in good agreement with the observed spectra (see Fig. 1).

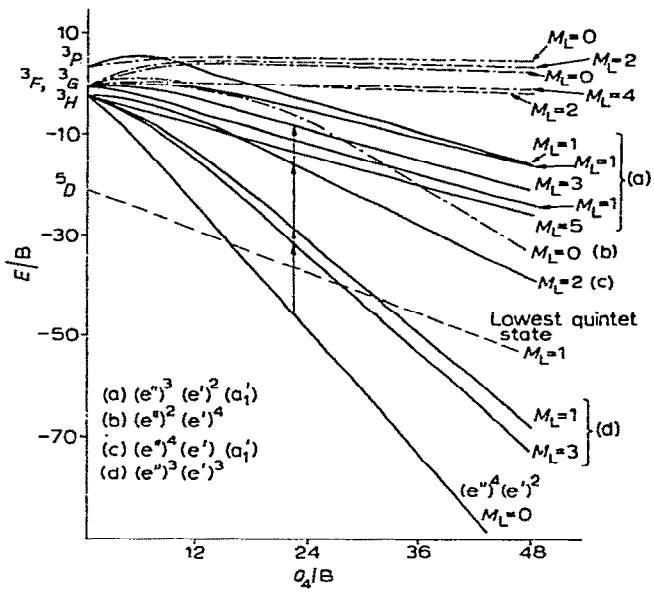

Fig. 9. Energy-level diagram for trigonal bipyramidal, low-spin complexes of iron(II), d^6, at $Q_2/Q_4 = 1.3$. (Reproduced by kind permission of the Chemical Society).

The spectra of the complexes of other d^8-metal ions, *e.g.*, in complexes of the types [RhX(QL)], $[M(CO)(QL)]^+$ (M = Co, Rh and Ir), (see Fig. 4), $[M(NCS)(QL)]^+$ (M = Ni, Pd and Pt), (see Fig. 5), and $[ML(QL)]^{2+}$ (M = Pd and Pt; L = uncharged ligand) resemble those of complexes [NiX(QL)]$^+$ (Ref. 6). On descending each sub-group the bands of analogous complexes shift towards higher energy and the shifts of the lowest energy absorption region are those expected for the general order of increasing ligand field splitting between the first, second and third transition series. On this basis, the lowest energy feature, when resolved from the charge-transfer bands, can be assigned to the transition $(e'')^4(e')^4 \rightarrow (e'')^4(e')^3(a'_1)^1$. This feature consists of a band on the high-energy side and a

shoulder on the low-energy side, separated by about 2000 cm^{-1}. The splitting has been attributed to a lowering of symmetry from C_{3v} to C_{2v} in the complexes on the grounds that in [PtI(QAS)] [BPh_4] the equatorial angles are 122, 119 and 103° (Ref. 6). In this context it is significant to note that this splitting occurs only in complexes of metal ions of the second and third transition series. Here the widening of bond angles may be due to the larger size of the metal ions. However, the possibility that such splitting may be due to spin-orbit coupling effects cannot be excluded.

Intensities of the ligand-field bands.—As all the QP and QAS complexes lack a centre of inversion, the intensities of the bands assigned to "ligand-field" transitions are likely to arise from the large mixing-in of higher configurations belonging both to excited states of the metal ions and to charge-transfer states by odd ligand-field components.

Charge-transfer bands.—All the complexes show two other high intensity bands, in some cases appearing only as shoulders, in the regions 28,000–31,000 cm^{-1} (see Figs. 1 to 5) and 37,000–39,000 cm^{-1} (see Fig. 3). The first band is tentatively assigned to phosphorus–metal (or arsenic–metal) charge-transfer and the second band may well be due to metal–X (X = anionic or other ligand) charge-transfer.

In conclusion, it is evident that the absorption spectra of trigonal bipyramidal complexes of QP and QAS can be interpreted satisfactorily using a ligand-field model as long as it is realized that this model is used in a purely formal sense. Thus, in the above treatment the effects of covalency, expected to be substantial in our complexes, are included in the parameters Q_2 and Q_4.

REFERENCES

1 M. CIAMPOLINI, N. NARDI AND G. P. SPERONI, *Coordin. Chem. Rev.*, 1 (1966) 222.
2 M. T. HALFPENNY, J. C. HARTLEY AND L. M. VENANZI, *J. Chem. Soc.*, (A) (1966) 627.
3 K. A. JENSEN AND C. K. JØRGENSEN, *Acta Chem. Scand.*, 19 (1965) 415.
4 L. M. VENANZI, *Angew. Chem., Int. Edn.*, 3 (1964) 453.
5 M. J. NORGETT, J. H. M. THORNLEY AND L. M. VENANZI, *J. Chem. Soc.*, (A) (1967) 540.
6 G. DYER AND L. M. VENANZI, *J. Chem. Soc.*, (1965) 2771.
7 C. J. BALLHAUSEN AND A. D. LIEHR, *J. Mol. Spectry.*, 2 (1958) 342.
8 M. T. HALFPENNY, J. G. HARTLEY AND L. M. VENANZI, *J. Chem. Soc.*, (A) (1967) 627.
9 D. G. E. KERFOOT AND L. M. VENANZI, unpublished observations.
10 R. J. MAWBY AND L. M. VENANZI, *Essays in Coordination Chemistry, Exper. Suppl. IX*, Birkhäuser, Basel, 1963, p. 240.
11 D. G. E. KERFOOT, R. J. MAWBY AND L. M. VENANZI, unpublished observations.
12 D. G. E. KERFOOT, J. G. HARTLEY AND L. M. VENANZI, unpublished observations.
13 G. DYER AND L. M. VENANZI, *J. Chem. Soc.*, (1965) 1293.
14 C. A. SAVAGE AND L. M. VENANZI, *J. Chem. Soc.*, (1962) 1548.
15 J. A. BREWSTER, C. A. SAVAGE AND L. M. VENANZI, *J. Chem. Soc.*, (1961) 3699.
16 G. DYER, J. G. HARTLEY AND L. M. VENANZI, *J. Chem. Soc.*, (1965) 1293.
17 I. V. HOWELL, L. M. VENANZI AND D. C. GOODALL, *J. Chem. Soc.*, (A) (1967) 395.
18 B. CHISWELL AND L. M. VENANZI, *J. Chem. Soc.*, (A) (1966) 417.

19 R. J. MAWBY AND L. M. VENANZI, *J. Chem. Soc.*, (1962) 4447.
20 J. G. HARTLEY, L. M. VENANZI AND D. C. GOODALL, *J. Chem. Soc.*, (1963) 3930.
21 E. KONIG AND H. L. SCHLAFER, *Z. Physik. Chem.*, 26 (1960) 371.
22 T. M. DUNN, R. S. NYHOLM AND S. YAMADA, *J. Chem. Soc.*, (1962) 1564.
23 G. DYER AND D. W. MEEK, *Inorg. Chem.*, 4 (1965) 1398.
24 G. DYER AND D. W. MEEK, *Inorg. Chem.*, 6 (1967) 149.